# Photorearrangements of Five 1- and 2-Naphthyl Acylates in Three Unstretched and Stretched Polyethylene Films. Does Reaction Selectivity Correlate with Free Volumes Measured by Positron Annihilation Lifetime Spectroscopy?

**Weiqiang Gu,[†,§] Anita J. Hill,[‡] Xiaochun Wang[⊥,†,] Changxing Cui,[†,#] and Richard G. Weiss*[,†]**

*Department of Chemistry, Georgetown University, Washington, D.C. 20057-1227, and CSIRO Manufacturing Science and Technology, Private Bag 33, Clayton South MDC, Victoria 3169, Australia, and Department of Chemistry, Monash University, Clayton, Victoria 3168, Australia*

*Received March 3, 2000; Revised Manuscript Received August 9, 2000*

ABSTRACT: The selectivity of photorearrangements of five 1-naphthyl and 2-naphthyl acylates has been investigated in three unstretched and stretched polyethylene films of different crystallinities and in isotropic solutions. The influence of variables such as size and position of the aryl groups of the esters, degree of crystallinity, free volume, and unstretched/stretched state of the films has been explored. The orthopositronium accessible free volume sites in the undoped unstretched and stretched polyethylenes have been measured by positron annihilation lifetime spectroscopy. These void free volumes are much smaller than the van der Waals volumes of the naphthyl molecules under investigation. The naphthyl esters inside polyethylene cavities act as templates for the formation of their photoproducts. Long alkyl chains on naphthyl myristates not only affect the shape anisotropy but also induce large van der Waals interactions with the walls of reaction cavities. Stretching enhances the templating effect and strengthens the van der Waals attractions with cavity walls in the case of naphthyl myristates, thus inducing marked increases in reaction selectivities in polyethylene films. Somewhat surprisingly, there is no correlation between void free volume of a host polyethylene film and selectivity of photoreactions of a guest naphthyl ester.

## Introduction

The concept of a "reaction cavity" was first introduced by Cohen to explain the selectivity of reactions occurring in the solid state.[1] Since then, it has been extended to many reaction types, including photochemical reactions in organized and constraining media.[2] In some cases, the natures of well-characterized reaction cavities can be used to learn how guest molecules are transformed to specific products. In others, well-understood transformations of guest molecules can provide insight into the natures of their reaction cavities. We differentiate reaction cavities (occupied sites) and "voids" (unoccupied sites) within media. Previously, we have attempted to correlate various properties of several polyethylene (**PE**) films[3] with the rates of diffusion[3,4] and reactivities[5] of small molecules within in them. Their accessible free volumes, considered a key factor, could only be estimated.[6] We also found that stretching **PE** films leads to lower rates of diffusion[7] and greater reaction selectivity[5] of guest molecules. This and related phenomena[8] strongly suggest that film stretching decreases the average free volume of individual reaction cavities in **PE**.

**PE** is a name given to literally hundreds of polymers of ethylene, as well as copolymers of ethylene and 1-alkenes, that differ in their degree of crystallinity, thermal and mechanical history, number and types of chain branches, degree and types of unsaturation, etc.[9] Degree of crystallinity is largely dependent upon the number and type of branches on the polymer chains.[10] **PE** can be divided roughly into low-density (**LDPE**; <50% crystallinity) and high-density classes (**HDPE**) which have a larger or smaller number of methyl groups per 1000 methylene units, respectively.[10] Microscopically, **PE** contains spherulites consisting of crystalline lamellae separated by amorphous regions.[11]

Photo-Fries[12] rearrangements in media of low polarity (like **PE**) proceed via homolytic bond scission to form a geminate radical pair (Scheme 1). Our inability to initiate reactions of both 1-naphthyl acetate (triplet state energy, $E_T$ = 289.5 kJ/mol[12a]) and 2-naphthyl acetate ($E_T$ < 259 kJ/mol[13,14]) from their excited triplet states upon sensitization by benzophenone ($E_T$ = 289.5 kJ/mol[15]) indicates that both bond scission and formation of the initial radical pair occur from an excited singlet state or, less likely, an upper triplet state.[13,16]

Here, we study photo-Fries rearrangements of five different 1-naphthyl acylates (**1**) and 2-naphthyl acylates (**2**) (Scheme 1 and eqs 1[16b,c] and 2[13] of Scheme 2) in three **PE** films in their unstretched and stretched states. Guest molecules such as **1** and **2** are located in the amorphous and interfacial regions (i.e., along the lateral faces of lamellae constituting microcrystallities) of the polymer.[17] Attempts are made to correlate various parameters of the model advanced by us previously for characterizing reaction cavities (i.e., their *free volume*, *shape*, and *wall stiffness*)[2a] with the course and selectivities of the rearrangements. In this way, we seek to

[†] Georgetown University.
[‡] CSIRO Manufacturing Science and Technology and Monash University.
[§] Current address: Department of Chemistry, University of California, Berkeley, CA 94720.
[⊥] Current address: U.S. Pharmacopeia,12601 Twinbrook Parkway, Rockville, MD 20852.
[#] Current address: Honeywell International, 101 Columbia Road, Morristown, NJ 07962-1021.

10.1021/ma000392u CCC: $19.00 © 2000 American Chemical Society
Published on Web 09/23/2000

**Scheme 1. Photo-Fries Rearrangements of Naphthyl Acylates**

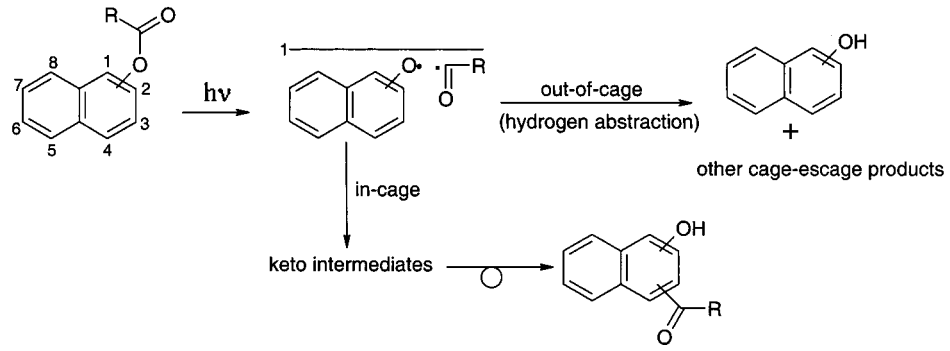


**Scheme 2**

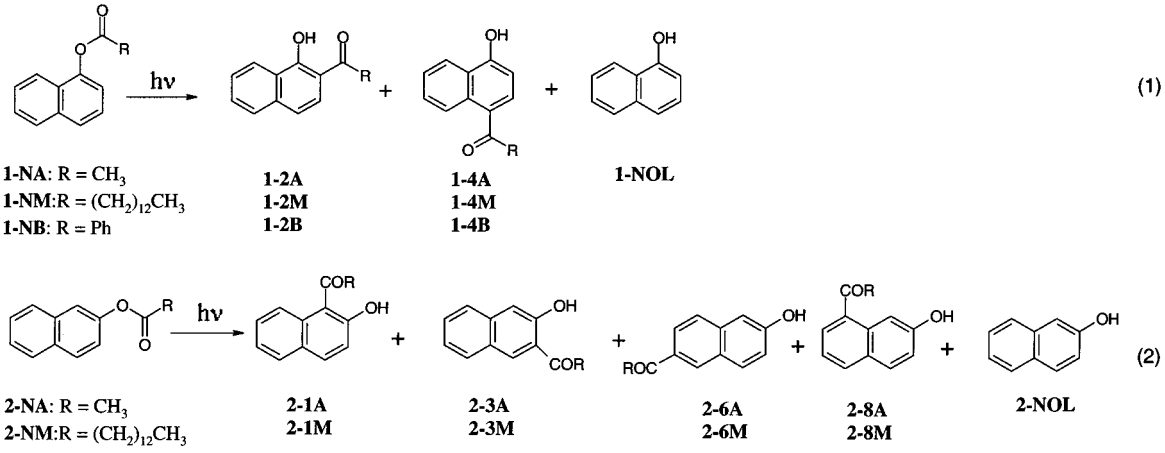


**Table 1. Polymer Crystallinity and oPs Lifetimes ($\tau_3$), Calculated Mean Void Radii ($R$), and Mean Free Void Volumes ($V_{PE}$) for Unstretched (u) and Stretched (s) PE Films**

| sample ID | $\tau_3$ (ns), ±0.024 ns | $R$ (Å) | $V_{PE}$ (Å$^3$) | % crystallinity (±2%)[a] | density (g/cm$^3$)[b] | C=C/1000CH$_2$[b] | CH$_3$/1000CH$_2$[b] |
|---|---|---|---|---|---|---|---|
| **BHDPE**(u) | 2.277 | 3.095 | 124 | 51 | 0.945 | 0 | 12 |
| **BHDPE**(s) | 2.162 | 3.000 | 113 | 52 | | | |
| **BLDPE**(u) | 2.445 | 3.234 | 142 | 24 | 0.917 | 0.38 | 41 |
| **BLDPE**(s) | 2.250 | 3.075 | 122 | 33 | | | |
| **NBLDPE**(u) | 2.444 | 3.234 | 142 | 26 | 0.916 | 0.33 | 21 |
| **NBLDPE**(s) | 2.270 | 3.092 | 124 | 33 | | | |
| **NDLDPE**(u) | 2.420 | 3.215 | 139 | 26 | 0.918 | 0.50 | 38 |
| **NDLDPE**(s) | 2.246 | 3.071 | 121 | 34 | | | |

[a] By differential scanning calorimetry (DSC). Previously reported crystallinities,[3] calculated from DSC data obtained with a less precise instrument, differ somewhat from the data presented here. [b] From ref 3.

identify the major factors contributing to control of guest molecule reactions in **PE** cavities. The walls of the **PE** reaction cages can be regarded as "passive" (i.e., very weakly interacting with the guest molecules and their intermediates).[2] However, in the presence of long alkyl chains on the acyl part of the naphthyl esters, van der Waals interaction may make the walls "active".

The naphthyl esters differ in size and shape. In each case, it is the location of the oxy radical center and the nature of the acyl group that distinguishes the singlet radical pairs in Scheme 1.

Many of the properties of the **PE** films employed here, except their orthopositronium (oPs) accessible void free volumes, have been reported previously (Table 1).[3] For completeness, the data include a fourth film whose oPs accessible void free volume has been determined by positron annihilation lifetime spectroscopy (PALS)[18] but has not been employed as a reaction medium. The effect of cold-stretching the films on their void free volumes (as perceived by electron densities) is also examined and compared with results from photo-Fries rearrangements.

Atomistic and molecular modeling techniques have been used to calculate the size distribution, shape, and dynamics of accessible free volume in polymers.[19a−e] The shape of the cavities is nonspherical with asphericity indicative of elongated voids or ellipsoids. The oPs accessible free volume measured by PALS has been compared to penetrant accessible free volumes calculated using molecular simulations.[19a] The conclusion drawn from these results is that the oPs probe and penetrants of van der Waals radii from 1.2 to 2.5 Å (and possibly larger) perceive the same characteristic cavities.[19a] Positron annihilation results for stretched polymers suggest cavity anisotropy indicative of ellipsoidal shapes.[20a,b] Empirical models that approximate the dimensions of spherical,[21a−c] ellipsoidal,[22] and cuboidal[23] free volumes from an oPs lifetime are used for comparative purposes to give qualitative information rather than quantitative predictions. We emphasize that the free

volumes studied by PALS are only those cavities accessible to oPs. As discussed by Ito,[24] oPs data as a probe of free volume must be interpreted with caution.

## Results

**Void Free Volumes of Sites and Degrees of Crystallinity of Unstretched and Stretched PE Films**. Few PALS studies have compared free volume changes between unstretched and stretched **PE** films.[25] Wang et al.[25a,b] measured the PALS of a cold-stretched film consisting of 80% **HDPE** and 20% **LDPE** at $\eta =$ 190% under fixed strain; strain $\eta(\%) = 100 \times (l - l_0)/l_0$, where $l_0$ and $l$ are the lengths of the sample before and after stretching, respectively. Hill et al.[25c] used extension under hydrostatic pressure at extrusion temperatures from 60 to 100 °C to achieve billets with very high draw ratios ($\eta \leq 1500\%$ before fracture). In both studies, the free volume probed by PALS increased initially and then decreased on further stretching. Prior studies using rheological and photochemical methods[7] indicate that film stretching reduces free volume. The present work examines the relationship in **PE** films between free volume in voids (i.e., unoccupied sites probed by PALS) and in occupied sites (according to photochemical selectivities). Attempts are made to discern which properties of the polymers have the greatest influence on the free volumes and reaction selectivities. These include cold stretching (to $\eta \cong 300\%$ for **LDPE**s and 400% for **BHDPE**) and degree of crystallinity.

In the PALS technique, an orthopositronium (**oPs**), the lightest possible atom (consisting of an electron and a positron with parallel spins),[26] probes the electron density of its immediate environment and, therefore, the free volume of "voids", through its annihilation catalyzed by interaction with electrons from the void walls (a "pick-off" annihilation). Sites with less free volume have higher local electron densities, resulting in shorter **oPs** lifetimes.[27]

In most polymers, there are three lifetime components in the positron annihilation lifetime decay. The longest-lived one, $\tau_3$, is from **oPs** pick-off annihilation. In the absence of special complications, $\tau_3$ is related to the radius $R$ of the cavity in which it resides by the semiempirical eq 3.[28] When the units of $\tau_3$ are nanoseconds, the units of $R$ are angstroms. The corresponding intensity $I_3$ is an indicator of the relative concentration of the voids. Since all of the voids in **PE** as assumed in eq 3 are not spherical and they exist in a distribution of sizes, $R$ provides the mean radii of the voids.

$$\tau_3 = \frac{1}{2}\left[1 - \frac{R}{R + 1.66} + \frac{1}{2\pi}\sin\frac{2\pi R}{R + 1.66}\right]^{-1} \qquad (3)$$

The $\tau_3$ and $I_3$ values of **BHDPE** and **NBLDPE** in their unstretched and stretched states are shown in Figures 1 and 2, respectively, as a function of $^{22}$Na source contact time. The **oPs** lifetimes are nearly constant, while intensities decreased with time. Interpretation of $I_3$ is complicated by its dependence on relative free-volume-void concentration and the probability of **oPs** formation. In some polymers, including **PE**, contact with the positron source reduces the formation probability over time by producing electron or positron scavengers; a logarithmic decrease in intensity as a function of contact time with a positron source for some polymers does not reflect a decrease in free volume. To avoid this problem, characteristic $I_3$ values are taken at early times, after 70 min of source contact.

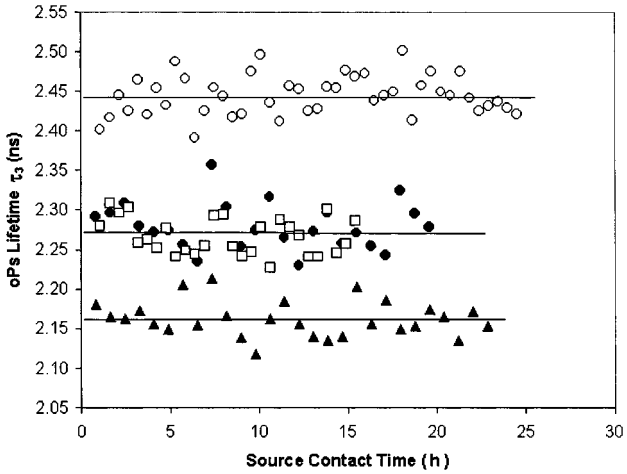


**Figure 1. oPs** lifetimes ($\tau_3$) as a function of source contact time for unstretched (u) and stretched (s) **PE** films: u (○) and s (□), **NBLDPE**; u (●) and s (▲), **BHDPE**.

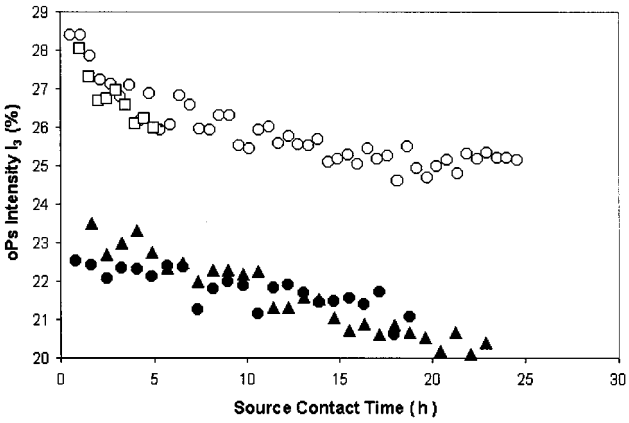


**Figure 2. oPs** intensity ($I_3$) as a function of source contact time for unstretched (u) and stretched (s) **PE** films: u (○) and s (□), **NBLDPE**; u (●) and s (▲), **BHDPE**.

Figure 3 shows the average values of $\tau_3$ and $I_3$ in our unstretched and stretched **PE** films. Note that (1) stretching caused decreases in $\tau_3$ in all four films, (2) $I_3$ remains almost constant upon stretching, indicating a constant concentration of holes, and (3) the film of highest crystallinity, **BHDPE**, has substantially lower $\tau_3$ and $I_3$ values than the three **PE**s of lower crystallinity. From eq 3, the measured $\tau_3$ values, and assuming spherical shapes, the radii of the voids and the corresponding mean free volumes ($V$) have been calculated (Table 1).

The crystallinities of the three unstretched **LDPE**s are similar and so are their free volumes. Upon film stretching, the crystallinities increased 7−8% and the free volumes decreased 18−20 Å$^3$. The free volume of unstretched **BHDPE** is smaller than those in unstretched **LDPE**s. Stretching caused no detectable change in crystallinity and a much smaller decrease of free volume, 11 Å$^3$.

The extent of morphological change induced by stretching is evident in DSC thermograms of a representative **LDPE**, **NBLDPE** (Figure 4), and **BHDPE** (Figure 5). The appearances of the curves from the **LDPE**s before and after stretching are similar, but the heat contents of the melting transitions of the stretched polymers are larger and the temperatures at maximum heat flow of

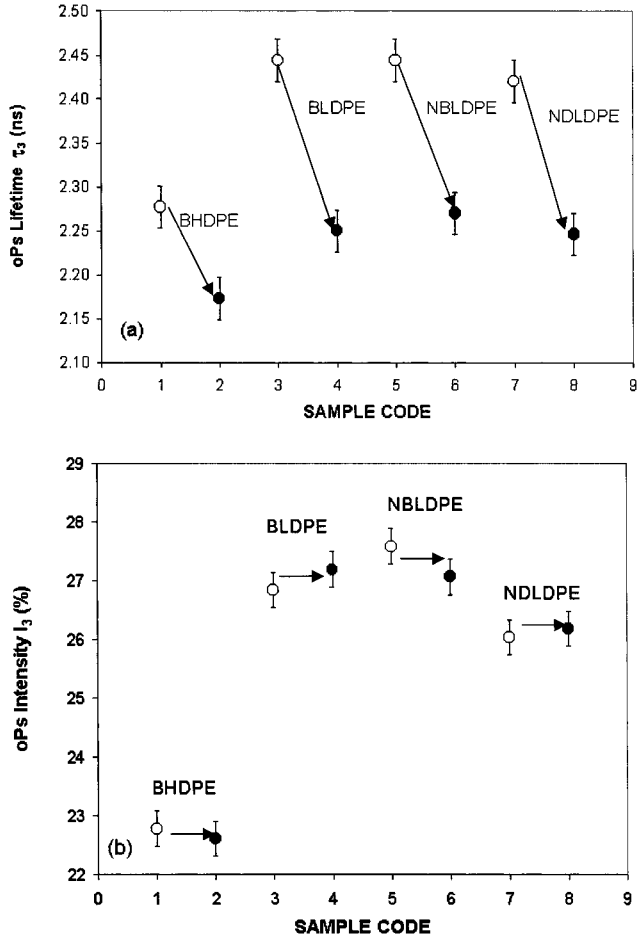


**Figure 3. oPs** pickoff lifetimes ($\tau_3$; a) and intensities ($I_3$; b) for unstretched (open symbols) and stretched (closed symbols) **PE** films.

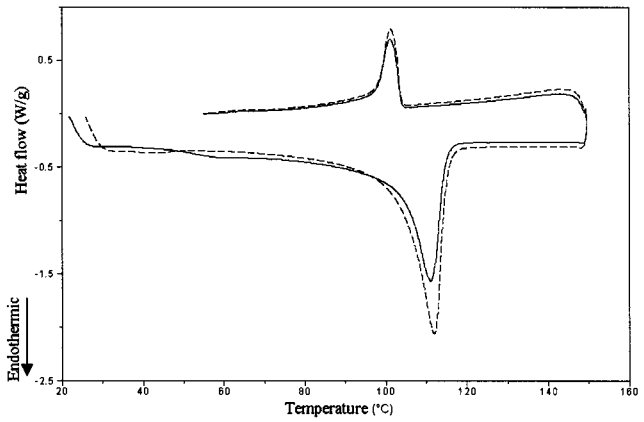


**Figure 4.** DSC thermograms of unstretched (—) and stretched (- - -) **NBLDPE** (first heating and cooling cycle).

the stretched polymers are 1−2 °C higher. The single melting transition of unstretched **BHDPE** is split into lower and higher temperature components upon stretching. During the second heating cycle of stretched **BHDPE** (not shown), only one endotherm (like the higher temperature component) was present. The first heating anneals the polymer.

**Photo-Fries Rearrangements of 2-Naphthyl Acylates**. Photo-Fries reactions of 2-naphthyl acylates have been examined in isotropic solutions,[13b,29] and some preliminary results in **PE** films have been reported.[13a] Table 2 lists the relative product distributions from

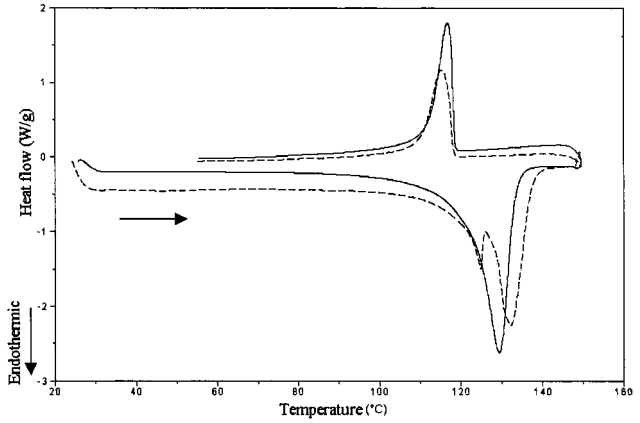


**Figure 5.** DSC thermograms of unstretched (—) and stretched (- - -) **BHDPE** (first heating and cooling cycle).

irradiations of 2-naphthyl acetate (**2-NA**) and 2-naphthyl myristate (**2-NM**) in two unstretched and stretched **PE** films, as well as in isotropic solutions. In isotropic solutions, 2-acyl-1-naphthols (**2**−**1**) are the major rearrangement products. Significant amounts of the cage-escape product, **2-NOL**, are present, also. The ability of the small acetyl radical from **2-NA** to diffuse easily from its initial reaction cage, even in the **PE** films, is indicated by the relatively large amounts of **2-NOL** that are found. In **PE** films, **2-1A** and **2-3A** are formed in comparable amounts from **2-NA**. By contrast, **2-3M** is the major product from irradiations of **2-NM** in **PE** films, and formation of **2-1M** is suppressed completely! Due to the much slower diffusion of a myristoyl radical than an acetyl radical, **2-NOL** from irradiations of **2-NM** was present in small amounts in the **PE** matrices; the low extinction coefficient of **2-NOL** at the wavelength of our HPLC detector (254 nm) is responsible for a rather high detection limit. The diffusion probability of a radical from its primary cage should be proportional to the inverse of square root of its molecular mass.[30] Thus, the much lower yield of cage-escape product from irradiation of **2-NM** than from irradiation of **2-NA** is expected.

Although film stretching increased **2-3A/2-6A** product ratios only slightly in **NDLDPE**, a much large effect is found in **BHDPE**. The **2-3M/2-6M** ratios were increased significantly upon stretching all of the **PE** films.

**Photo-Fries Rearrangements of 1-Naphthyl Acylates**. In previous work with 2-naphthyl esters, we have demonstrated that photo-Fries rearrangements are from in-cage radical coupling.[13] Similar results are found upon irradiation of 1-naphthyl benzoate (**1-NB**) in hexane and in some **PE** films. Specifically, no benzil, a product expected from dimerization of two benzoyl radicals from out-of-cage combination, was detected. The nearly constant ratio of 2- to 4-position photo-Fries products from irradiation of 1-naphthyl phenylacetate in hexane in the presence of wide range of thiophenol concentrations also supports in-cage recombination mechanism of acyl/1-naphthoxy radical pairs.[16c]

Photoproduct distributions from irradiations of 1-naphthyl acetate (**1-NA**), 1-naphthyl benzoate (**1-NB**), and 1-naphthyl myristate (**1-NM**) in isotropic solutions and **PE** media are summarized in Table 3. The number of photoproducts from irradiations of the 1-naphthyl esters is smaller than that from the 2-naphthyl esters. The cage-escape product **1-NOL** is present in detectable quantities only during irradiations of **1-NA** in hexane

**Table 2. Relative Photoproduct Yields from Irradiations of 2-Naphthyl Acylates in Isotropic Solutions and in Unstretched (u) and Stretched (s) Polyethylene Films at 25 °C**

| ester | conversion (%) | medium | conc[a] | 2−1 | 2−3 | 2−6 | 2−3/2−6 | 2-NOL[c] |
|---|---|---|---|---|---|---|---|---|
| **2-NA** | 16 | *tert*-butyl alcohol | 5 | 34 ± 1 | 15 ± 1 | 14 ± 1 | 2.4 | 37 ± 3 |
| | 11 | hexane | 5 | 57 ± 2 | 16 ± 1 | 6 ± 3 | 9.5 | 21 ± 2 |
| | 10−11 | **NDLDPE**(u) | 11 | 38 ± 2 | 17 ± 1 | 22 ± 2 | 0.77 | 23 ± 3 |
| | 9−12 | **NDLDPE**(s) | 16 | 31 ± 2 | 21 ± 1 | 17 ± 2 | 1.2 | 31 ± 5 |
| | 7−10 | **BHDPE**(u) | 11 | 21 ± 4 | 29 ± 5 | 21 ± 3 | 1.4 | 29 ± 5 |
| | 8−20 | **BHDPE**(s) | 9.5 | 20 ± 4 | 66 ± 4 | ≤2 | >33 | ≤12 |
| **2-NM** | 9 | *tert*-butyl alcohol[b] | 5 | 64 ± 2 | 14 ± 1 | 8 ± 1 | 1.8 | 12 ± 5 |
| | 5 | hexane | 5 | 43 ± 2 | 32 ± 2 | 8 ± 1 | 4.0 | 15 ± 6 |
| | 2−4 | **NDLDPE**(u) | 13 | 0 | 85 ± 2 | 10 ± 2 | 8.9 | ≤5 |
| | 5−7 | **NDLDPE**(s) | 13 | 0 | >90 | ≤1 | >90 | ≤10 |
| | 2−3 | **BHDPE**(u) | 31 | 0 | 83 ± 2 | 12 ± 2 | 6.9 | ≤5 |
| | 8−12 | **BHDPE**(s) | 10 | 0 | 94 ± 3 | ≤1 | >94 | ≤5 |

[a] mM in isotropic solvents and mmol/kg in **PE** films. [b] ca. 3% of **2−8M** detected also. [c] Limit of detection was 5%.

**Table 3. Relative Photoproduct Yields from Irradiations of 1-Naphthyl Acylates in Hexane and in Unstretched (u) and Stretched (s) Polyethylene Films at 22 °C**

| ester | conv (%) | medium | conc[a] | 1−2 | 1−4 | 1−2/1−4 | 1-NOL[d] |
|---|---|---|---|---|---|---|---|
| **1-NA** | 7 | hexane[b] | 1.0 | 28.0 ± 0.4 | 31.2 ± 0.4 | 0.9 | 40.8 ± 0.2 |
| | 9 | **NDLDPE**(u)[b] | 4.0 | 77.8 ± 0.5 | 15.0 ± 0.3 | 4.2 | 8.2 ± 0.4 |
| | 8 | **NDLDPE**(s)[b] | 4.0 | 77.8 ± 0.4 | 15.9 ± 0.5 | 4.9 | 6.3 ± 0.4 |
| | 2 | **NBLDPE**(u) | 1.0 | 73.7 ± 1.3 | 26.3 ± 1.0 | 2.8 | <2 |
| | 8 | **NBLDPE**(s) | 1.0 | 77.8 ± 1.1 | 22.2 ± 0.3 | 3.9 | <2 |
| | 9 | **BHDPE**(u)[b] | 3.0 | 78.1 ± 0.2 | 16.1 ± 0.4 | 4.9 | 5.8 ± 0.3 |
| | 6 | **BHDPE**(s)[b] | 3.0 | 76.8 ± 0.2 | 13.1 ± 0.4 | 5.9 | 10.1 ± 0.4 |
| **1-NB** | 2 | hexane | 2 | 78.3 ± 3.3 | 21.7 ± 0.9 | 3.6 | <2 |
| | 5 | **NDLDPE**(u) | 5 | 86.7 ± 4.6 | 13.3 ± 0.7 | 6.5 | <2 |
| | 5 | **NDLDPE**(s) | 7 | 86.1 ± 2.8 | 13.9 ± 0.4 | 6.2 | <2 |
| | 6 | **NBLDPE**(u) | 6 | 86.8 ± 3.3 | 13.2 ± 0.5 | 6.6 | <2 |
| | 7 | **NBLDPE**(s) | 7 | 86.7 ± 2.0 | 13.3 ± 0.3 | 6.5 | <2 |
| | 3 | **BHDPE**(u) | 6 | 88.8 ± .1 | 11.2 ± 0.8 | 7.9 | <2 |
| | 3 | **BHDPE**(s) | 6 | 88.2 ± 0.7 | 11.8 ± 0.8 | 7.5 | <2 |
| **1-NM** | 7 | hexane | 1.1 | 4.0 ± 0.1 | 3.0 ± 0.1 | 1.3 | <2 |
| | 9 | *tert*-butyl alcohol[c] | 1.2 | 100 | <1 | >100 | <2 |
| | 4 | **NDLDPE**(u) | 2.3 | 100 | <1 | >100 | <2 |
| | 4 | **NDLDPE**(u) | 4.2 | 100 | <1 | >100 | <2 |
| | 4 | **BHDPE**(u) | 1.1 | 100 | <1 | >100 | <2 |

[a] mM in isotropic solvents; mmol/kg in **PE** films. [b] At 20 °C. [c] At 26 °C. [d] Detection limit was 2%.

and some of the **PE** films. These results are consistent with those from **2-NA** and the high mobility of acetyl radicals, regardless of their origin.

The ratios of the two rearrangement products, **1-2/1-4**, in **PE** are at least twice that in hexane. In **PE** films **1-2A/1-4A** ratios increase slightly with increasing crystallinity or upon stretching; **1-2B/1-4B** ratios do not change appreciably when **PE** films are stretched. Apparently, the natures of the **PE** cages have little influence on the fates of these acyl/1-naphthoxy radical pairs. Irradiation of **1-NM**, generating a very large and less mobile myristoyl radical, yields no discernible **1-4M** in either of the two **PE** films employed or in the polar solvent, *tert*-butyl alcohol. Only in the nonpolar, low-viscosity solvent, hexane, does the myristoyl/1-naphthoxy radical pair have sufficient mobility and space to allow formation of **1-4M**. Experiments in stretched **PE** films with **1-NM** were not performed because of the absence of any products besides **1-2M** in the unstretched ones. The reaction cages of unstretched **PE** already control the fates of the radical pairs from **1-NM**.

## Discussion

**PALS and DSC Studies on the Consequences of Film Stretching**. A series of PALS studies on **PE** have been performed recently.[6,25a,31] Our PALS results from unstretched **PE** films indicates that free volume of **PE** voids decrease with increasing crystallinity. The same conclusion has been reached by Serna et al.[6] Although the effect of cold stretching on the free volume **PE** voids has been studied by Wang et al.,[25a,b] their focus was mainly on the stretching protocol, and a film consisting of a blend of low- and high-density **PE**s was employed. The results reported here appear to be the first extensive studies on free volume changes in voids upon cold stretching **PE** to their fracture limit. In each case, stretching decreases the void free volume while the concentration of voids remains almost constant. The decreased free volume of stretched **PE** may be related to better alignment of polymer chains in the amorphous regions. A more parallel local arrangement of chains permits stronger van der Waals attractions between methylene units and, consequently, reduces the average separation. Furthermore, stretching increased the crystallinity of each of the **LDPE**s examined. Although stretching does not increase the crystallinity of **BHDPE**, it can affect the morphology by changing the distribution of crystallites and the relative volume fraction of interfacial regions. Such changes are indicated by Figure 5 and the significant differences between photoproduct ratios of some naphthyl acylates (N.B., **2-NA**) from unstretched and stretched **BHDPE**.

**Reaction Cavity Interactions Are Expressed as the Photochemistry of 1 and 2**. In order for a singlet radical pair in Scheme 1 to yield a keto (product) isomer, there must be motion of an acyl radical with respect to its naphthoxy partner. In isotropic media, like hexane, the question of which radical moves is moot. However,

in viscous anisotropic media like **PE** films, it is not because motion of each radical within or with respect to its reaction cage has different experimental consequences. For instance, the presence of **NOL** (i.e., a cage-escaped product) in product mixtures from irradiations of both **NA** isomers, combined with its absence upon irradiations of **1-NB** and the **NM** isomers, strongly suggests that the small radical is the primary migrating species in reaction cages occupied by acetyl/naphthoxy pairs. If naphthoxy radicals were able to move easily within the films **1-NB** and the **NM** isomers should also have yielded significant quantities of **NOL**. Furthermore, the absence of appreciable quantities of cage-escape product from irradiation of **1-NB** in the **PE** films coupled with the lack of sensitivity of **1-2/1-4** ratios to **PE** stretching or crystallinity indicates that the benzoyl/1-naphthoxy radical pairs are able to move a great deal with respect to each other within their reaction cages, but they are not able to escape from them before combining. When viewed as a set, the **1-2/1-4** photoproduct ratios from the three esters of **1** indicate that the selectivity of the motions available to acyl/1-naphthoxy radical pairs in their **PE** reaction cages depend on the size of the acyl moiety. As the van der Waals volume of the acyl group increases, so do the **1-2/1-4** ratios. Since formation of the keto precursor of **1**−**2** involves less motion by the radical pair than does formation of the keto precursor of **1**−**4** (due to the lysis step placing the acyl group near the naphthoxy oxygen atom on carbon-1), either attenuated intracage diffusion (a kinetic effect) or a lack of adequate free volume near carbon-4 of the 1-naphthoxy ring system (steric effect) may be responsible for the observed trends in photoproduct selectivity. These factors will be considered later.

The presence of **2-1A** and absence of **2-1M** from irradiations of **2-NA** and **2-NM**, respectively, in all of the **PE** films indicates that the nature of the reaction cage can help to direct the mechanistic courses of the radical pairs. The 1-isomer is the major product from both 2-naphthyl esters in hexane, and the distance necessary for an acyl radical to travel from the point of its creation (at the naphthoxy oxygen atom on carbon-2) to the 1- or 3-position of the naphthoxy ring is virtually the same; there is no *intra*molecular reason for the decrease or complete loss of **2-1** products (and consequent increase in **2-3** and **2-6** products) in **PE** films. The cause must be *supra*molecular (i.e., related to the interaction of the radical pairs with their reaction cages).

There may be more than one supramolecular factor operative. For instance, electronic interactions between the cavity walls and specific groups of **1** and **2** or their radical pair intermediates may influence conformations and trajectories of motion. Also, steric factors related to the size and shape of the reaction cavities may enhance selected reaction pathways if the cavity walls are "stiff" (i.e., their relaxation times are longer than the lifetimes of the radical pairs from irradiation of **1** and **2** and the esters consume all of the volume within a cavity).

Wall interactions may be very important in directing photorearrangements of the **NM** isomers. van der Waals interactions between the long myristoyl groups and the polyethylene chains that constitute the walls of the reaction cavities may be very strong. Assuming parallel close packing between myristoyl and polyethylene chains and 2 kcal/mol as the interaction energy per methylene unit,[32] the total attraction may be >20 kcal/mol!

In essence, dispersion forces may glue the myristoyl radical to its initial position for the duration of the radical pair lifetime within a **PE** reaction cage. If correct, the rotational mobility of the naphthoxy radical and, perhaps, the conformational liability of the one or two methylene groups closest to the acyl radical center will determine whether any **1-4M** (from **1-NM**) or **2-6M** (from **2-NM**) can be formed. Clearly, such an anchoring effect to cavity walls cannot occur with acetyl or benzoyl radicals.

Second, the shape anisotropy of the reaction cage is greatest for **NM** isomers and smallest for the **NA** isomers if, as we suspect, the esters are a shape template for their reaction cages. In other work, we have provided strong arguments that relaxation of the chains constituting the reaction cavity walls in **PE** occurs in the same time frame or more slowly than acyl/naphthoxy singlet radical pairs react.[16c,33] On this basis, the keto intermediate of the photo-Fries product that will be formed preferentially is the one that is most similar in shape to its precursor ester and involves the least motion of the radical pair. The degree to which this template affect will be manifested depends, as mentioned, upon the shape anisotropy of the initial ester: **NM** > **NB** > **NA**. In the most severe cases, stretched **PE** films containing **1-** or **2-NM**, the only photo-Fries product detected places the acyl group at a carbon atom of the naphthyl ring that is adjacent to the naphthoxy oxygen atom.

The discussion above does not explain why the major photoproduct from **2-NM** in an isotropic, nonpolar solvent (hexane) and an isotropic, polar, H-bonding solvent (*tert*-butyl alcohol) is so disfavored in all of the **PE** films. There is a glaring preference for **2-3M** over **2-1M**, although both should involve similar amounts of radical pair motion to be formed. A possible reason may due to a second form of wall−guest interactions. From data by Michl and Thulstrup,[34] the long molecular axis of naphthalene makes an angle of ca. 50° with respect to the polyethylene chains that flank it. If a similar oblique angle is preferred between the naphthyl parts of **2-NM** and their neighboring polyethylene chains, and if the myristoyl chains are "anchored" to the walls through van der Waals interactions, the cavity will direct the reaction to the 3-position of the naphthoxy ring. Similarly, longitudinal diffusion by the myristoyl chain over the 2-naphthyl ring system will allow reaction at position-6 (and formation of **2-6M**). Film stretching may block this diffusional mode by reducing the free volume available along the axis orthogonal to the naphthyl ring. Analogous "anchoring" orientations of **1-NM** in unstretched **PE** films do not direct the myristoyl radical center to the reactive 4-position of a 1-naphthoxy radical. Without some rotation of the 1-naphthoxy rings with respect to the axis defined by the myristoyl chain (or vice versa), no **1-4M** is expected, and none is detected even in unstretched **PE** films. The more mobile (less anchored) acetyl and benzoyl radicals from **1-NA** and **1-NB**, respectively, are able to explore a greater amount of space and approach the 4-position of 1-naphthoxy to effect reactions.

**The Influence of PE Crystallinity on Photoproduct Ratios.** If **PE** crystallinity is the most important parameter in determining the characteristics of the reaction cavities offered to **1** and **2**, it should be possible

**Table 4. Calculated van der Waals Volumes of Naphthyl Acylates ($V_M$)[29] (in Parentheses) and $\Delta V$, the Differences between $V_M$ and the Appropriate Mean Void Free Volume ($V_{PE}$) from Table 1 for Unstretched (u) and Stretched (s) PE Films; All Units Are in Å$^3$**

| ester ($V_M$) | **1-NA** (166) | **2-NA** (166) | **1-NB** (220) | **1-NM** (370) | **2-NM** (370) |
|---|---|---|---|---|---|
| $V_M - V_{\mathbf{NBLDPE}(u)}$ | 24 | 24 | 78 | 228 | 228 |
| $V_M - V_{\mathbf{NBLDPE}(s)}$ | 42 | 42 | 96 | 246 | 246 |
| $V_M - V_{\mathbf{NDLDPE}(u)}$ | 27 | 27 | 81 | 231 | 231 |
| $V_M - V_{\mathbf{NDLDPE}(s)}$ | 45 | 45 | 99 | 249 | 249 |
| $V_M - V_{\mathbf{BHDPE}(u)}$ | 42 | 42 | 96 | 246 | 246 |
| $V_M - V_{\mathbf{BHDPE}(s)}$ | 53 | 53 | 107 | 257 | 257 |

to correlate the photoproduct ratios from one ester and degree of crystallinity from various unstretched and stretched **PE** films. A perusal of the data in Tables 1−3 immediately demonstrates that no such correlation occurs. For instance, the crystallinities of unstretched **NBLDPE** and **NDLDPE** are nearly the same and smaller than that of **BHDPE**. Yet, there are discernible difference between **1-2/1-4** ratios from **1-NA** in the two **LDPE**s and the ratios from **1-NB** and **1-NM** are independent of crystallinity. Similarly, the **2-3/2-6** ratio from **2-NA** is smaller in unstretched **NDLDPE** than in unstretched **BHDPE**; the opposite trend applies to the photoproduct ratios from **2-NM**. Although the photoproduct ratios from **2** increase with crystallinity when one unstretched and stretched **PE** film are compared, they do not when **1-NB** is irradiated. Crystallinity may play a secondary role in determining photoproduct selectivities (i.e., formulating the nature of reaction cavities), but it appears to have no direct influence on the course of the photoreactions of **1** and **2**. In retrospect, this conclusion may have been predicted since the naphthyl esters do not enter the crystalline regions of **PE** films.[17a]

**The Influence of $\Delta V$ on Photoproduct Ratios.** As shown in Table 4, van der Waals volumes[35] of **1** and **2** are always larger than the void free volumes in **PE** films as measured by PALS. Clearly, free volume in reaction cavities is an important determinant of photorearrangement selectivities. Although free volume in voids (the only sites monitored by PALS) and in occupied reaction cavities cannot be compared directly, $\Delta V$, the volume difference between the van der Waals volume of a guest molecule ($V_M$) and the void free volume of **PE** ($V_{PE}$) from PALS (Table 4), may reflect the environmental compression experienced by naphthyl acylates in **PE** reaction cages. If so, $\Delta V$ may correlate with changes in photoproduct ratios listed in Tables 2 and 3.

However, we find no obvious general relationship. For the same ester examined in different **PE**s, there is no direct correlation between $\Delta V$ and photoproduct ratios. In some cases, similar values of $\Delta V$ lead to quite different photoproduct ratios from one naphthyl ester (such as **2-NM**), and in others, different values of $\Delta V$ lead to similar photoproduct ratios (such as **1-NB**). Although the **1-2A/1-4A** and **2-3A/2-6A** ratios, from **1-NA** and **2-NA**, respectively, change with $\Delta V$, there is no obvious proportionality.

**The Influence of Film Stretching on Product Ratios**. When a film is stretched, the ratios of **1-2A/1-4A** and **2-3A/2-6A** from **1-NA** and **2-NA**, respectively, increase. The enormous increase in **2-3A/2-6A** when **BHDPE** is stretched is not found in the photoproduct ratios from **1-NA**. Furthermore, stretching of **BHDPE** induces a decrease in **2-NOL** from **2-NA** and an increase in **1-NOL** from **1-NA**!

The unexpected increase in out-of-cage reaction from **1-NA** upon film stretching and the very small increase in the **1-2A/1-4A** ratios indicate that the reaction cavities afforded to **1-NA** and **2-NA** by **BHDPE** are somewhat different, and they continue to be different when these films are stretched. Clearly, these differences cannot be correlated with $\Delta V$ since the values for **1-NA** and **2-NA** are the same. As mentioned, they may be related to orientations of the naphthyl rings with respect to the polyethylene chains of the reaction cavity walls[34] and the subsequent effect the different locations of the acetyl radicals will have in the cages immediately after lysis from the excited singlet states.

## Conclusions

The photochemistries of the esters do not correlate with $\Delta V$. The most obvious example of the lack of sensitivity of photoproduct ratios to $\Delta V$ is provided by **1-NB**! On the basis of the PALS-derived void free volumes, none of the naphthyl esters employed here should be incorporated into **PE** films. Our doping method, swelling of the **PE** matrices, softens the walls and enlarges the sizes of voids, allowing them to accept molecules such as **1** and **2**. As the swelling liquid is removed (and the walls harden) via its rapid diffusion, the molecules of **1** and **2** are trapped in sites that are no longer typical of the voids in native **PE** films. In essence, the guest molecules serve as templates to create their own reaction cavities. The shape and size of each cavity are determined by the specific shape and size of the large molecule residing within it. This concept has been exploited for different purposes in different polymers by Shea and co-workers.[36]

There are consequences of introducing large guest molecules into a polymer on the remaining (unoccupied) voids. The recent study by Huang et al.[37] on the effect of temperature on chromophore-doped poly(methyl methacrylate) presents a somewhat analogous situation to our stretching experiments. They found that introduction of azobenzene molecules in poly(methyl methacrylate) (PMMA) increased the mean void cavity size. This may be expected since the azobenzene molecules are much larger than the intrinsic voids of PMMA. A solvent-casting or related method must be used to incorporate the guests into the polymer films. However, the **oPs**-measured mean free volume cavity size decreased to below that found in undoped PMMA when films were annealed for extended periods above $T_g$. It is our view that the thermal energy associated with annealing allowed the large guest molecules to force polymer chains of their cavity walls, and other chains in the vicinity, to become closer.

In our experiments, conducted isothermally (at room temperature), strain energy from film stretching results in constraints applied by polymer chains of the reaction cavities on motions of guest molecules. As a result, selectivity of photoreactions is altered. Although we have shown that strain energy can be used to reduce the void size in the absence of the guest molecule, there is no obvious quantitative correlation between the change in void free volume of undoped films due to stretching and reaction selectivity. Thus, an a priori assessment of the quantitative effect of film stretching on the selectivity of reaction of a guest molecule is not possible.

Even in some of the experiments with **1** and **2** in which no large changes in photoproduct ratios ac-

**Table 5. Two Longest oPs Lifetimes ($\tau_3'$, $\tau_4'$) from Four Exponent Fits to PALS Data and the Related Intensities ($I_{3'}$, $I_{4'}$), and Calculated Mean Void Radii ($R$) for Unstretched (u) and Stretched (s) PE Films**

| sample ID | $\tau_{3'}$ (ns) ± 0.13 | $R$ (Å) | $I_{3'}$ (%) ± 1.0 | $\tau_{4'}$ (ns) ± 0.05 | $R$ (Å) | $I_{4'}$ (%) ± 1.3 |
|---|---|---|---|---|---|---|
| **BHDPE**(u) | 1.263 | 2.05 | 8.78 | 2.692 | 3.42 | 14.01 |
| **BHDPE**(s) | 1.143 | 1.88 | 7.57 | 2.424 | 3.22 | 16.81 |
| **BLDPE**(u) | 1.634 | 2.49 | 9.84 | 2.862 | 3.54 | 16.52 |
| **BLDPE**(s) | 1.530 | 2.38 | 11.42 | 2.638 | 3.38 | 17.36 |
| **NBLDPE**(u) | 1.671 | 2.53 | 10.59 | 2.881 | 3.56 | 16.94 |
| **NBLDPE**(s) | 1.481 | 2.32 | 9.81 | 2.600 | 3.35 | 17.26 |
| **NDLDPE**(u) | 1.576 | 2.43 | 9.22 | 2.808 | 3.50 | 16.41 |
| **NDLDPE**(s) | 1.472 | 2.31 | 6.73 | 2.480 | 3.26 | 19.69 |

companied film stretching, the cages may have been altered perceptibly. Employing another ester, 1-naphthyl 2-phenylpropanoate, as the probe, we have examined the kinetics of the in-cage radical pair recombination process shown in Scheme 1.[16d] The activation energies for formation of the corresponding **1-2** and **1-4** are nearly twice as large in stretched **NDLDPE** as in the unstretched film. Furthermore, activation energies are significantly larger in unstretched **BHDPE** than in unstretched **NDLDPE**. Both of these results demonstrate that the mean free void volumes affect the reaction kinetics in ways that may not be discernible from isothermal comparisons.

Our model for the effect of strain energy on reaction cages in **PE** films predicts that there is little excess free volume in occupied sites and that their shape is determined by the shape and orientation of the guest molecule with respect to polyethylene chains of the cavity walls. During the transformation of the guest to its photoproducts, it is the stiffness of the polyethylene chains (i.e., the hardness of the walls) combined with how strongly they interact anisotropically with parts of the guest molecule (as in the case of directional van der Waals attractions to long myristoyl chains and naphthyl rings) that controls the ability of selective transformations to occur. Our PALS data indicate that film stretching exacerbates motional constraints imposed on guest molecules by their reaction cavities in **PE** by reducing the total available void volume within a film, but overall, no one property of a **PE** film (e.g., void volume or degree of crystallinity) is a quantitative predictor of the influence that a **PE** film will exert on the selectivity of a guest molecule's reactions. However, these factors and others dealing with the shape and interaction anisotropy of guest molecules with the walls of their reaction cavities do allow qualitative predictions to be made.

In this regard, the consequences of (macroscopic) film stretching on (microscopic) molecular reactivity have been demonstrated to be very important. Morphologically, stretching **PE** films redistributes more evenly microcrystallites within the amorphous domains and increase overall crystallinity (especially when the degree of crystallinity is initially low). Others[17] and we[16c,38] have presented evidence that the mole fraction of guest molecules at the interfacial sites increases (at the expense of amorphous sites) when a film is stretched. However, our work indicates that the majority of guest molecules continue to reside in amorphous **PE** reaction cavities even after film stretching.[16c]

Distinguishing interfacial and amorphous free volume sites in **PE** has been attempted by Kindl and Reiter[39] using a four-component fit to PAL spectra. The two longer-lived components, $\tau_{3'}$ and $\tau_{4'}$, are attributed to **oPs** at crystalline−amorphous interfaces and in amorphous regions, respectively. A four-exponent model of our PALS data (Table 5) gave fits with higher variance and higher standard deviations than the three-component fit. The large standard deviations on the components (i.e., $I_{3'}$ and $I_{4'}$) make the change in the relative population of the sites on stretching unclear. The deviations are due to the decreases in $I_{3'}$ and $I_{4'}$ as a function of source contact time.

Unfortunately, the poor fits to a four-exponential decay model bring its validity here into question. Regardless, interpretation of our PALS results in the Kindl−Reiter framework suggests that there is a smaller number of interfacial than amorphous voids (and reaction cavities) in both the unstretched and stretched films. In addition, the size of both types of site decreases on stretching. The mean free void volumes of the interfacial sites, calculated from the $\tau_{3'}$ values in Table 5, are exceedingly small. They range from 68 Å$^3$ (unstretched **NBLDPE**) to 28 Å$^3$ (stretched **BHDPE**). On this basis, interfacial sites at which molecules of **1** or **2** reside do not resemble voids in the native films. By contrast, the mean free void volumes of amorphous sites, calculated from the $\tau_{4'}$ values in Table 5, are much larger than those based upon a three-exponential decay fit (Table 1 and $\tau_3$). The smallest, 140 Å$^3$ (from stretched **BHDPE**), and the largest, 189 Å$^3$ (from unstretched **NBLDPE**), are slightly smaller and larger, respectively, than the van der Waals volumes of the **NA** esters. We conclude that the number of interfacial voids is smaller than the amorphous ones and that both interfacial and amorphous cavities decrease in size on stretching. Even if the Kindl−Reiter model is correct here, the very small sizes and much smaller numbers of interfacial sites argue against a large fraction of the naphthyl esters residing there. A quantitative assessment is possible only if the probability of formation of oPs and subsequent processes occur with the same efficiency in amorphous and interfacial regions. However, the relative probabilities and efficiencies are not known.

We favor the single reaction cavity type model (for each ester) based upon the better mathematical fit using three exponential terms for PALS data, the insensitivity of the relative photoproduct yields to conversion of the esters, and Ockham's razor. The results indicate that only one family of reaction cages per **PE** film need be invoked to explain the changes in the photochemistry of each naphthyl acylate irradiated, regardless of the model selected.

## Experimental Section

**Instrumentation**. UV/vis absorption spectra were recorded on a Perkin-Elmer Lambda-6 spectrophotometer. For measurement of dopant concentrations in **PE** films, a blank film was used as reference. IR spectra were recorded on a MIDAC FT-IR spectrometer using KBr pellets or a 1 mm liquid cell with NaCl windows. $^1$H NMR spectra were obtained on a Bruker 270 MHz NMR spectrometer with a Tecmag operating

system or a Varian Mercury 300 MHz NMR spectrometer interfaced to a Sun SparcStation 5. Differential scanning calorimetry (DSC) was conducted under a slow stream of nitrogen on a TA 2910 instrument interfaced to a TA Thermal Analyst 3100 controller. The heating rate was 10 °C/min, and the cooling rate, although uncontrolled, was slower than the heating rate. Melting points (corrected) were determined on a Leitz SM-LUX-POL microscope with a Leitz 585 thermostating stage and a NiCr−NiAl thermocouple. GC-MS was performed on a FISONS MD-800 GC-MS instrument with a 0.25 $\mu$m Alltech DB-5 (15 m × 0.25 mm) column.

High-performance liquid chromatography (HPLC) analyses employed a Waters chromatograph with a UV detector (254 nm), an electronic integrator, and either an Alltech 250 × 4.4 mm 5$\mu$ silica gel column (column A) or an Alltech 250 × 4.4 mm 5$\mu$ $C_{18}$ column (column B). For **1-NM** analyses, column A and 15/1 (v/v) hexane/ethyl as eluent; for **1-NB** analyses, column B and 2/1 (v/v) acetonitrile/water as eluent; for **1-NA** analyses, column A and 15/1/1 (v/v/v) hexane/ethyl acetate/methanol as eluent; for **2-NM** analyses, column A and methylene chloride as eluent; for **2-NA** analyses, either column A and 15/1 (v/v) hexane/ethyl acetate as eluent or column B and 1/2 (v/v) acetonitrile/water as eluent.

Positron annihilation lifetime spectra were collected using an automated EG&G Ortec fast-fast coincidence system, temperature stabilized at 22.5 ± 1 °C. The timing resolution of the system, 275 ps, was determined using the prompt curve from a $^{60}$Co source with energy windows set to $^{22}$Na events. **PE** films were stacked to a thickness of 1.5 mm on either side of a $^{22}$Na source. The source gave a two-component best fit to 99.99% pure annealed aluminum (169 ± 2 ps, 99.3 ± 0.3%; 820 ps, 0.7%), and no source correction was used in the analysis. Approximately 30 sequential spectra were collected for each sample; each spectrum took approximately 35 min to collect 30 000 peak counts (or 1 million integrated counts). Each spectrum could be fitted well by the sum of three exponential terms. Spectra were analyzed using PFPOSFIT[40] with the shortest lifetime fixed at 0.125 ns. The lifetime of the long-lived component, $\tau_3 = \tau_{oPs}$, did not change with source contact time. The intensity of the long-lived component, $I_3 = I_{oPs}$, was a function of source contact time as reported previously for **PE**s.[41]

**Reagents**. Solvents for HPLC analyses and photoreactions were HPLC or spectroscopy grade and were used as received. 1-Naphthyl acetate (ACROS, 99%) was sublimed under vacuum at ca. 100 °C to yield white crystals, mp 45−46 °C (lit.[42] mp 45−46 °C). 1-Naphthol (Aldrich, 99%) was dissolved in 20% aqueous NaOH, precipitated by acidifying with concentrated HCl, recrystallized from hexane, and sublimed under vacuum at ca. 100 °C to yield white crystals; mp 95−96 °C (lit.[43] mp 94 °C). 2-Acetyl-1-naphthol (Aldrich, 99%), mp 97−98 °C (lit.[44] mp 98−99 °C), was obtained as pale yellow crystals after recrystallization from hexane. 1,2-Diphenylethane (99%) and benzopinacol (99%) were used as received from Aldrich. Benzhydrol (Aldrich, 99%; from petroleum ether) and benzophenone (Aldrich, 99%; from benzene) were recrystallized. *tert*-Butyl alcohol (99%; Fisher) was distilled before use. Photoproducts from **2-NA** and **2-NM** have been reported previously and were available from previous studies.[13b]

The **PE** films have been characterized previously:[3] **BLDPE** (additive-free, type NA-203) and **NBLDPE** (additive-free, type NA-677) were from Poliolefinas, Brazil, **BHDPE** (type ES-300) was from Polialden Petroquimica, Brazil, and **NDLDPE** was from DuPont of Canada. They were immersed sequentially in three chloroform aliquots for 1 week to remove additives, dried, and stored under a nitrogen atmosphere until used. Films were cold-stretched slowly by hand to ca. 4 (**LDPE**s) or 5 (**BHDPE**) times their original length.

**Film Doping Procedures**. Doping was achieved by placing strips of film in hexane (**1**) or chloroform (**2**) solutions containing ca. 0.1 M ester in the dark for 24−48 h. The films were dried under a stream of nitrogen, washed with acetonitrile to remove any surface-occluded naphthyl acylate, wiped gently with a tissue, and then dried with a stream of nitrogen. The resulting dopant concentrations in unstretched films were determined from UV/vis absorption spectroscopy and Beer's law using averaged optical densities of at least three different parts of each film, the film thickness,[3] and the appropriate molar extinction coefficients ($\epsilon$) at 254 nm: in hexane, 2400 (**1-NA**), 2300 (**1-NB**), and 3500 (**1-NM**) $M^{-1}$ $cm^{-1}$; 3400 $M^{-1}$ $cm^{-1}$ for both **2-NM** (in 1/100 (v/v) ethyl acetate/hexane) and **2-NA** (in 1/15 (v/v) ethyl acetate/hexane).

**Irradiation Procedures.** Films were placed in closed Pyrex glass containers, purged with nitrogen for about 15 min, and irradiated on both faces for the same length of time under nitrogen. Liquid solutions were bubbled with $N_2$ for 15 min and irradiated under a $N_2$ atmosphere. Samples at nonambient temperatures were irradiated in sealed Pyrex vessels while thermostated in a Haake FK-2 constant temperature (±1 °C) water bath. The UV radiation source (>300 nm) was the water- and Pyrex-filtered output of either a 450 W Hanovia medium-pressure mercury lamp or an HBO 500W/2L2 Oriel 6285 mercury lamp operated at 200−400 W.

**Product Analyses**. Irradiated films were kept in the dark while immersed in aliquots of chloroform (6 h each) until no starting material and/or photoproducts could be extracted (by HPLC and/or GC analyses). The combined aliquots were concentrated carefully under reduced pressure before being analyzed.

Photoproducts were identified in HPLC analyses by their retention times and overlap of peaks during co-injections of reaction mixtures with authentic samples. Integrated peak areas ($A_i$) were converted to relative concentrations ($C_i$) and yields ($Y_i$) by correcting for different $\epsilon_i$ values in the eluting solvent. The extinction coefficients of 1-naphthyl and 2-naphthyl acylates and their corresponding photoproducts are listed in supplementary Tables 1 and 2, respectively.

The relative photoproduct yields of **1** in both isotropic solutions and in **PE** films (Tables 3) and **2** in isotropic solutions (Table 2) are averages of three HPLC analyses at a specified conversions. The relative photoproduct yields of **2** in **PE** films (Table 2) are the averages from at least six separate analyses (≥2 runs and ≥3 chromatograms/run); precision errors are one standard deviation. The yields showed no systematic deviations within the range of conversions investigated.

**Crystallinity of Stretched PE Films**. The heats of melting ($\Delta H$) of both unstretched and stretched films of same type were measured sequentially by DSC. The crystallinity was calculated using 286 J/g as the value of the heat of melting for 100% crystalline **PE**.[45] Some differences were found between the heats of melting ($\Delta H$) measured here and previously using a less sophisticated DSC instrument.[3]

**Crossover Experiments.** Solutions containing **2-NM** (5 mM) and 7-methoxy-2-naphthyl acetate (5 mM) were irradiated at >300 nm[13b] in nitrogen saturated *tert*-butyl alcohol. Photoproducts were analyzed by HPLC. No **2-NA**, 3-acetyl-2-naphthol, or 1-acetyl-2-naphthol was detected. In a separate experiment, 7-methoxy-2-naphthyl acetate was shown to be photoreactive in the same solvent. In addition, irradiations of **1-NB** in isotropic solution and in **PE** films (Table 3) yielded no detectable benzil.

**Syntheses**. **4-Acetyl-1-methoxynaphthalene.** Powdered dry aluminum chloride (35 g, 0.26 mol) was added to a vigorously stirred mixture of acetyl chloride (19 mL, 0.26 mol) and carbon tetrachloride (50 mL). When it cooled to 20 °C, 1-methoxynaphthalene (18 mL, 0.12 mol) in carbon tetrachloride (50 mL) was added, and the mixture was warmed to 30 °C while hydrogen chloride gas was removed under aspirator pressure. After 30 min, crushed ice (~200 mL) was added, the mixture was filtered, and the solid was washed with carbon tetrachloride (100 mL). The combined filtrates were extracted with dilute HCl (2 × 50 mL), 5% aqueous $Na_2CO_3$ (100 mL), and water (3 × 100 mL) and then dried ($MgSO_4$). The liquid was reduced to a residue, which was recrystallized from 100 mL of hexane to yield colorless crystals (24 g, 92%); mp 70−72 °C (lit.[46] mp 72 °C). $^1$H NMR ($CDCl_3$/TMS): 9.0 (d, $J$ = 8.8 Hz, 1H, naphthyl), 8.2 (d, $J$ = 8.4 Hz, 1H, naphthyl), 7.9 (d, $J$ = 7.9 Hz, 1H, naphthyl), 7.6 (t, $J$ = 7.0 Hz, 1H, naphthyl), 7.5 (t, $J$ = 7.0 Hz, 1H, naphthyl), 6.8 (d, $J$ = 8.4 Hz, 1H, naphthyl),

4.0 (s, 3H, $-OCH_3$), 2.6 ppm (s, 3H, $-COCH_3$); mass *m*/*z* calcd for $C_{13}H_{12}O_2$ 200, found 200.

**4-Acetyl-1-naphthol.** 4-Acetyl-1-methoxynaphthalene (1.0 g, 5.0 mmol) and pyridine hydrochloride[47] (3.0 g, 26 mmol) were heated at 200 °C for 3 h under a dry atmosphere. At room temperature, 20 mL of 5% aqueous HCl was added. The mixture was filtered, dissolved in ethyl acetate (20 mL), and dried ($MgSO_4$). Solvent was removed and the residue was recrystallized from 20 mL of 1/15 (v/v) ethyl acetate/hexane to yield 0.42 g (44%) of white crystals; mp 197.5−198.5 °C (lit.[42] mp 198 °C). $^1$H NMR ($CDCl_3$/TMS): 9.03 (d, $J$ = 8.8 Hz, 1H, naphthyl), 8.27 (d, $J$ = 8.4 Hz, 1H, naphthyl), 7.95 (d, $J$ = 7.9 Hz, 1H, naphthyl), 7.64 (t, $J$ = 7.0 Hz, 1H, naphthyl), 7.54 (t, $J$ = 7.0 Hz, 1H, naphthyl), 6.82 (d, $J$ = 8.4 Hz, 1H, naphthyl), 6.47 (b, 1H, −OH), 2.71 ppm (s, 3H, $-COCH_3$); mass *m*/*z* calcd for $C_{12}H_{10}O_2$ 186, found 186.

**1-Naphthyl Myristate.** 1-Naphthol (7.0 g, 49 mmol) and myristoyl chloride (15 mL, 55 mmol) were dissolved in benzene (20 mL) and refluxed for 3 h under a dry atmosphere. At room temperature, chloroform (50 mL) and water (100 mL) were added. The organic layer was separated, extracted with water (100 mL), saturated aqueous $NaHCO_3$ (2 × 100 mL), and distilled water (100 mL), and dried ($MgSO_4$). The residue (after evaporation) was recrystallized from cyclohexane to yield 15.2 g (88%) of white crystals; mp 54−56 °C. $^1$H NMR ($CDCl_3$/TMS): 7.89−7.22 (m, 7H, naphthyl), 2.73 (t, $J$ = 7.5 Hz, 2H, $-CO-CH_2-$), 1.86(q, $J$ = 7.2 Hz, 2H, $-CO-CH_2-\mathit{CH_2}-$), 1.55−1.27 (m, $-(CH_2)_{10}-$), 0.88 ppm (t, $J$ = 7.0 Hz, 6.6 Hz, 3H, $-CH_3$); mass *m*/*z* calcd for $C_{24}H_{34}O_2$ 354, found 354.

**2-Myristoyl-1-naphthol.** 1-Naphthyl myristate (5.0 g, 14 mmol) in pentane (25 mL) was cooled in an ice bath, and anhydrous $AlCl_3$ (5.0 g, 38 mmol) was added slowly. The mixture was refluxed for 30 min under a dry atmosphere and then cooled to room temperature. Ice-cooled hydrochloric acid (15%, 50 mL) and methylene chloride (50 mL) were added separately. The organic layer was extracted with water (50 mL), 10% aqueous NaOH (50 mL), and brine solution (2 × 50 mL) and then dried (MgSO4). The residue, after evaporation, was recrystallized from hexane to yield 2.0 g (40%) of a pale yellow solid; mp 94−96 °C. $^1$H NMR ($CDCl_3$/TMS): 14.16 (s, 1H, OH), 8.87−6.79 (m, 6H, naphthyl), 3.04 (t, $J$ = 7.5 Hz, 2H, $-CO-CH_2-$), 1.79(m, $-CO-CH_2-\mathit{CH_2}-$), 1.44−1.26 (m, $-(CH_2)_{10}-$), 0.88 ppm (t, $J$ = 6.9 Hz, 6.9 Hz, 3H, $-CH_3$). IR (KBr): 3247 (OH), 2945−2849 (CH, aliphatic), 1627 (C═O), 1464, 1390 (CH, aliphatic) cm$^{-1}$.

**1-Methoxy-4-myristoylnaphthalene.** Anhydrous $AlCl_3$ (9 g, 68 mmol) was added slowly to an ice-cooled solution of 1-methoxynaphthalene (12 g, 76 mmol), myristoyl chloride (15 mL, 55 mmol), and chloroform (40 mL), and the mixture was stirred for 24 h at room temperature under a dry atmosphere. Ice-cooled hydrochloric acid (15%, 100 mL) was added dropwise. The organic layer was extracted with saturated aqueous $NaHCO_3$ (100 mL) and brine solution (2 × 200 mL) and dried ($MgSO_4$). The residue, after evaporation, was recrystallized from 1-butanol to yield 23 g (83%) of white crystals; mp 61−62 °C. $^1$H NMR ($CDCl_3$/TMS): 8.84 (d, $J$ = 7.8 Hz, 1H, naphthyl), 8.31 (d, $J$ = 6.0 Hz, 1H, naphthyl), 7.95 (d, $J$ = 8.4 Hz, 1H, naphthyl), 7.61 (t, $J$ = 6.9 Hz, 1H, naphthyl), 7.51 (t, $J$ = 6.6 Hz, 1H, naphthyl), 6.80 (d, $J$ = 8.4 Hz, 1H, naphthyl), 4.06 (s, 3H, $-OCH_3$), 3.02 (t, $J$ = 7.5 Hz, 2H, $-CO-CH_2$), 1.78-(m, 2H, $-CO-CH_2-\mathit{CH_2}-$), 1.41−1.25 (m, $-(CH_2)_{10}-$), 0.88 ppm (t, $J$ = 6.9 Hz, 3H, $-CH_3$). IR (KBr): 2952−2848 (CH, aliphatic), 1669 (C═O), 1472 (CH, aliphatic), 1230 (C−O) cm$^{-1}$.

**4-Myristoyl-1-naphthol.** 1-Methoxy-4-myristoylnaphthylene (1.0 g, 5.0 mmol) and pyridine hydrochloride[47] (3.0 g, 26 mmol) were heated at 200 °C for 3 h under a dry atmosphere. At room temperature, 20 mL of 5% aqueous HCl was added, and the mixture was filtered. The solid was dissolved in ethyl acetate (20 mL), dried ($MgSO_4$), and reduced to residue. White crystals (0.42 g, 44%), mp 177−178 °C, were obtained upon recrystallization from 1/15 (v/v) ethyl acetate/hexane. $^1$H NMR ($CDCl_3$/TMS): 8.84 (d, $J$ = 8.7 Hz, 1H, naphthyl), 8.30 (d, $J$ = 7.5 Hz, 1H, naphthyl), 7.95 (d, $J$ = 8.4 Hz, 1H, naphthyl), 7.61 (t, $J$ = 6.9 Hz, 1H, naphthyl), 7.51 (t, $J$ = 6.6 Hz 1H, naphthyl), 6.79 (d, $J$ = 8.4 Hz, 1H, naphthyl), 3.02 (t, $J$ = 7.5 Hz, 2H, $-CO-CH_2$), 1.78(m, 2H, $-CO-CH_2-\mathit{CH_2}-$), 1.41−1.25 (m, $-(CH_2)_{10}-$), 0.88 ppm (t, $J$ = 6.9 Hz, 3H, $-CH_3$); mass *m*/*z* calcd for $C_{12}H_{10}O_2$ 354, found 354.

**1-Naphthyl Benzoate.** 1-Naphthol (7.3 g, 0.05 mol) was dissolved in 40 mL of cold 5% aqueous NaOH, and benzoyl chloride (5.8 mL, 0.05 mol) was added. The flask was shaken vigorously for 20 min and then cooled in an ice bath. The solid was filtered and washed with cold water (100 mL); it became an oil at room temperature. It was dissolved in ethyl acetate (50 mL), extracted with 5% aqueous NaOH (50 mL) and water (3 × 50 mL), and dried ($MgSO_4$). The liquid residue, after removal of the solvent under reduced pressure, was passed through a silica gel column (15/1 (v/v) hexanes/ethyl acetate) to yield 9 g (73%) of a white solid; mp 57 °C (lit. mp 56 °C,[48] 56.5−57.0 °C[49]). $^1$H NMR ($CDCl_3$/TMS): 7.29−8.36 ppm (m, aromatic). IR (KBr): 1729 cm$^{-1}$.

**4-Benzoyl-1-methoxynaphthalene.** Powdered dry $AlCl_3$ (35 g) was added to a vigorously stirred solution of benzoyl chloride (30 mL, 0.26 mol) in carbon tetrachloride (50 mL). The flask was immersed in a water bath at 20 °C, and a solution of 1-methoxynaphthalene (18 mL, 0.12 mol) in carbon tetrachloride (50 mL) was added. After stirring and heating at 30 °C for 30 min, ∼200 g of crushed ice was added. The mixture was filtered and the solid was washed with carbon tetrachloride (100 mL). The combined liquids were extracted with dilute aqueous HCl (2 × 50 mL), 5% aqueous $Na_2CO_3$ (100 mL), and water (3 × 100 mL) and dried ($MgSO_4$). The residue after evaporation of solvent was crystallized from hexane to obtain 28 g (90%) of colorless crystals; mp 112−113 °C. $^1$H NMR ($CDCl_3$/TMS): 8.37 (m, 2H, naphthyl), 7.84 (m, 2H, naphthyl), 7.42−7.61 (m, 6H, naphthyl), 6.80 (d, $J$ = 7.9 Hz, 1H, naphthyl), 4.08 ppm (s, 3H, $-0CH_3$). IR (KBr): 1642 (C═O), 1251 (C−O) cm$^{-1}$.

**4-Benzoyl-1-naphthol.** 4-Benzoyl-1-methoxynaphthalene (1.0 g, 3.8 mmol) and pyridine hydrochloride (3.0 g, 26 mmol) were heated at 200 °C for 3 h under a dry atmosphere. At room temperature, 20 mL of 5% aqueous HCl was added, and the mixture was filtered. The solid was dissolved in ethyl acetate (20 mL) and dried ($MgSO_4$). The residue, after removal of solvent, was recrystallized from 1/15 (v/v) ethyl acetate/hexane to yield 0.7 g (74%) of white crystals; mp 170−172 °C (lit.[50] mp 163−164 °C). $^1$H NMR ($CDCl_3$/TMS): 8.36 (m, 1H, naphthyl), 8.28 (m, 1H, naphthyl), 7.83 (d, $J$ = 7.0 Hz, 1H, aromatic), 7.42−7.61 (m, 6H, naphthyl), 6.78 (d, $J$ = 7.9 Hz, 1H, naphthyl). IR (KBr): 3312 (OH), 1630 (C═O) cm$^{-1}$.

**2-Benzoyl-1-naphthol.** 1-Naphthyl benzoate (6.0 g, 24 mmol), dry $AlCl_3$ (3.6 g, 27 mmol), and 60 mL of $CS_2$ were stirred and refluxed under a dry atmosphere for 2 days. The $CS_2$ was distilled, 20 mL of 17% HCl was added, and the aqueous phase was extracted with ether (3 × 50 mL). The combined ether layers were washed with saturated $NaHCO_3$ (3 × 50 mL) and water (3 × 50 mL) and dried ($MgSO_4$). After removal of solvent (rotary evaporator), the red oil residue was chromatographed on a silica gel column ($CHCl_3$). 2-Benzoyl-1-naphthyl and starting material eluted together. They were dissolved in hexanes containing a small amount of ethyl acetate and stirred overnight with 15% aqueous NaOH. The solid suspended between the layers was filtered under vacuum and washed with 15% aqueous NaOH. The combined aqueous parts were cooled in an ice bath, and 6 M HCl was added dropwise to pH 7. The resulting solid was eluted on a silica gel column (2% ethyl acetate in hexane) to yield 0.7 g (11%) of a yellow solid; mp 66.3−68.4 °C (lit.[51] mp 64−65 °C). $^1$H NMR ($CDCl_3$/TMS): 7.21−8.54 (m, 12 H, aromatic), 13.95 (s, 1 H, −OH). IR (KBr): 3458 (s and b), 1735 cm$^{-1}$.

**Acknowledgment.** The Georgetown group is grateful to the National Science Foundation and the Petroleum Fund (administered by the American Chemical Society) for their support of this research.

**Supporting Information Available:** Two tables of molar extinction coefficients at 254 nm for reactants and photoprod-

ucts in the HPLC eluent solvents. This material is available free of charge via the Internet at http://pubs.acs.org.

## References and Notes


(1) Cohen, M. D. *Angew. Chem., Int. Ed. Engl.* **1975**, *14*, 386.
(2) (a) Weiss, R. G.; Ramamurthy, V.; Hammond, G. S. *Acc. Chem. Res.* **1993**, *26*, 530. (b) Ramamurthy, V., Ed. *Photochemistry in Organized and Constrained Media*; VCH: New York, 1991. (c) Zimmerman, H. E.; Alabugin, I. V.; Chen, W.; Zhu, Z. *J. Am. Chem. Soc.* **1999**, *121*, 11930.
(3) Zimerman, O. E.; Cui, C.; Wang, X.; Atvars, T. D.; Weiss, R. G. *Polymer* **1998**, *39*, 1177.
(4) Taraszka, J. A.; Weiss, R. G. *Macromolecules* **1997**, *30*, 2467.
(5) (a) Ramesh, V.; Weiss, R. G. *Macromolecules* **1986**, *19*, 1486. (b) Tung, C.-H.; Yuan, Z.-Y.; Wu, L.-Z.; Weiss, R. G. *J. Org. Chem.* **1999**, *64*, 5156.
(6) Serna, C.; Abbe, J. Ch.; Duplatre, G. *Phys. Status Solidi A* **1989**, *115*, 389.
(7) (a) Naciri, J.; Weiss, R. G. *Macromolecules* **1989**, *22*, 3928. (b) He, Z.; Hammond, G. S.; Weiss, R. G. *Macromolecules* **1992**, *25*, 1568.
(8) (a) Talhavini, M.; Atvars, T. D. Z.; Schurr, O.; Weiss, R. G. *Polymer* **1998**, *39*, 3221. (b) Talhavini, M.; Atvars, T. D. Z.; Cui, O.; Weiss, R. G. *Polymer* **1996**, *37*, 4365.
(9) (a) Axelson, D. E.; Levy, G. C.; Mandelkern, L. *Macromolecules* **1979**, *12*, 41. (b) Quirk, R. P.; Alsamarraie, M. A. A. In *Polymer Handbook*; Brandrup, J., Immergut, E. H., Eds.; Wiley: New York, 1989; p V/15. (c) Hadley, D. W. In *Structure and Properties of Oriented Polymers*; Ward, I. M., Ed.; Wiley: London, 1975; Chapter 9. (b) Glenz, W.; Peterlin, A. J. *Macromol. Sci. Phys.* **1970**, *B4*, 473.
(10) (a) Brydson, J. A. *Plastic Materials*; Van Nostrand: London, 1966. (b) Crompton, T. R. *The Analysis of Plastics*; Pergamon: Oxford, 1984.
(11) (a) Geil, P. H. *Polymer Single Crystals*; Wiley: New York, 1963. (b) Wunderlich, B. *Macromolecular Physics*; Academic Press: New York, 1974; Vol. I.
(12) (a) Bellus, D. *Adv. Photochem.* **1971**, *8*, 109 and references therein. (b) Nakagaki, R.; Hiramatsu, M.; Watanabe, T.; Tanimoto, Y. *J. Phys. Chem.* **1985**, *89*, 3222. (c) Kalmus, C. E.; Hercules, D. H. *J. Am. Chem. Soc.* **1974**, *96*, 449. (d) Meyer, J. W.; Hammond, G. S. *J. Am. Chem. Soc.* **1970**, *92*, 2189.
(13) (a) Cui, C.; Weiss, R. G. *J. Am. Chem. Soc.* **1993**, *115*, 9820. (b) Cui, C.; Wang, X.; Weiss, R. G. *J. Org. Chem.* **1996**, *61*, 1962.
(14) Marchetti, A. P.; Kearns, D. R. *J. Am. Chem. Soc.* **1967**, *89*, 768.
(15) Leigh, W.; Arnold, D. R. *J. Chem. Soc., Chem. Commun.* **1980**, 406.
(16) (a) Stratenus, L. Ph.D. Thesis, University of Leiden, Leiden, The Netherlands, 1966 (cited as ref 8 in ref 12a). (b) Gu, W.; Warier, M.; Ramamurthy, V.; Weiss, R. G. *J. Am. Chem. Soc.* **1999**, *121*, 9467. (c) Gu, W.; Weiss, R. G. *Tetrahedron*, in press. (d) Gritsan, N. P.; Tsentalovich, Y. P.; Yurkovskaya, A. V.; Sagdeev, R. Z. *J. Phys. Chem.* **1996**, *100*, 4448.
(17) (a) Phillips, P. J. *Chem. Rev.* **1990**, *90*, 425 and references therein. (b) Jang, Y. T.; Phillips, P. J.; Thulstrup, E. W. *Chem. Phys. Lett.* **1982**, *93*, 66. (c) Meirovitch, E. *J. Phys. Chem.* **1984**, *88*, 2629. (d) Radziszewski, J. G.; Michl, J. *J. Phys. Chem.* **1981**, *85*, 2934.
(18) (a) Brandt, W., Dupasquier, A., Eds.; *Positron Solid-State Physics*; North-Holland: Amsterdam, 1983. (b) Schrader, D. M., Jean, Y. C., Eds.; *Positron and Positronium Chemistry*; Elsevier: Amsterdam, 1988.
(19) (a) Greenfield, M. L.; Theodorou, D. N. *Macromolecules* **1993**, *26*, 5461. (b) Misra, S.; Mattice, W. L. *Macromolecules* **1993**, *26*, 7274. (c) Rigby, D.; Roe, R. J. *Macromolecules* **1990**, *23*, 5312. (d) Arizzi, S.; Mott, P. H.; Suter, U. W. *J. Polym. Sci., Part B* **1992**, *30*, 415. (e) Theodorou, D. N. In *Diffusion in Polymers*; Neogi, P., Ed.; Marcel Dekker: New York, 1996; pp 67−142.
(20) (a) Jean, Y. C.; Nakanishi, H.; Hao, L. Y.; Sandreczki, T. C. *Phys. Rev. B* **1990**, *42*, 9705. (b) Jean, Y. J.; Rhee, Y.; Lou, Y.; Shelby, D.; Wilkes, G. L. *J. Polym. Sci., Part B* **1996**, *34*, 2979.
(21) (a) Tao, S. J. *J. Chem. Phys.* **1972**, *56*, 5499. (b) Eldrup, M.; Lightbody, D.; Sherwood, J. N. *Chem. Phys.* **1981**, *63*, 51. (c) Nakanishi, H.; Wang, S. J.; Jean, Y. C. In *International Symposium on Positron Annihilation Studies of Fluids*; Sharma, S. C., Ed.; World Scientific: Singapore, 1987; p 292.
(22) Jean, Y. C.; Shi, H. *J. Non-Cryst. Solids* **1994**, *806*, 172.
(23) Jasinska, B.; Koziol, A. E.; Goworek, T. *J. Radioanal. Nucl. Chem.* **1996**, *210*, 617.
(24) Ito, Y. In *Structure and Properties of Glassy Polymers*; Tant, M. R., Hill, A. J., Eds.; ACS Symposium Series Vol. 710; Oxford Books: New York, 1998; pp 334−354.
(25) (a) Wang, B.; Wang, C. L.; Li, S. Q.; Wang, S. J. *Phys. Status Solidi A* **1994**, *144*, 263. (b) Wang, S. J.; Wang, C. L.; Wang, B. *J. Phys. IV, Colloq. C4* **1993**, *3*, 275. (c) Hill, A. J.; Bastow, T. J.; Hodge, R. M. In *Structure and Properties of Glassy Polymers*; Tant, M. R., Hill, A. J., Eds.; American Chemical Society: Washington, DC, 1998; p 286. (d) Shelby, M. D. Ph.D. Dissertation, Virginia Polytechnic Institute and State University, Blackburg, 1996.
(26) Ache, H. J. In *Positronium and Muonium Chemistry*; Gould, R. F., Ed.; American Chemical Society: Washington, DC, 1979; Chapter 1.
(27) (a) Brandt, W.; Berko, S.; Walker, W. W. *Phys. Rev.* **1960**, *120*, 1289. (b) Eldrup, M.; Lightbody, M.; Sherwood, J. N. *Chem. Phys.* **1981**, *63*, 51.
(28) Nakanishi, H.; Wang, S. J.; Jean, Y. C. In *Positron Annihilation Studies of Fluids*; Sharma, S. C., Ed.; World Science: Singapore, 1998; p 292.
(29) Molokov, I. F.; Tsentalovich, Y. P.; Yurkovskaya, A. V.; Sagdeev, R. Z. *J. Photochem. Photobiol. A: Chem.* **1997**, *110*, 159.
(30) Guillet, J. In *Advances in Photochemistry*; Volman, D. H., Hammond, G. S., Gollnick, K., Eds.; Wiley: New York, 1988; Vol. 14, p 91.
(31) Prooijen, M. V.; Jorch, H. H.; Stevens, J. R.; Rudin, A. *Polymer* **1999**, *40*, 5111.
(32) (a) Abdallah, D. A.; Bachman, R. E.; Perlstein, J.; Weiss, R. G. *J. Phys. Chem. B* **1999**, *103*, 9269. (b) Israelachvili, J. N. *Intermolecular and Surface Forces*, 2nd ed.; Academic Press: New York, 1992; Chapter 11.
(33) The relaxation times of occupied sites in polyethylene are difficult to estimate because the size and shape of each guest will influence the chain segments constituting its host cage differently. However, the NMR determined correlation time of C−H dipolar interactions in the amorphous regions of polyethylene is ca. 50 ns [Tai, Y.; Okazaki, M.; Toriyami, K. *J. Chem. Soc., Faraday Trans.* **1992**, *88*, 23]. The correlation time of pyrene, which is expected to disturb its cage environment much more than molecules of the naphthyl acetates and benzoate, is ca. 2 orders of magnitude shorter than that of its host, an ethylene−propylene rubber.
(34) Michl, J.; Thulstrup, E. W. *Acc. Chem. Res.* **1987**, *20*, 192.
(35) Bondi, A. *J. Phys. Chem.* **1964**, *68*, 441.
(36) Hart, B. R.; Rush, D. J.; Shea, K. J. *J. Am. Chem. Soc.* **2000**, *122*, 460.
(37) Huang, C.-M.; Hellmuth, E. W.; Jean, Y. C. *J. Phys. Chem. B* **1998**, *102*, 2474.
(38) (a) Naciri, J.; Weiss, R. G. *Macromolecules* **1989**, *22*, 3928. (b) He, Z.; Hammond, G. S.; Weiss, R. G. *Macromolecules* **1992**, *25*, 1568. (c) Jenkins, R. M.; Hammond, G. S.; Weiss, R. G. *J. Phys. Chem.* **1992**, *96*, 496.
(39) Kindl, P.; Reiter, G. *Phys. Status Solidi A* **1987**, *104*, 707.
(40) Puff, W. *Comput. Phys. Commun.* **1983**, *30*, 359.
(41) Welander, M.; Maurer, F. H. J. *Mater. Sci. Forum* **1992**, *105−110*, 1811.
(42) Crouse, D. J.; Hurlbut, S. L.; Wheeler, D. M. S. *J. Org. Chem.* **1981**, *46*, 374.
(43) Chattaway, F. D. *J. Chem. Soc.* **1931**, 2495.
(44) Stoughton, R. W. *J. Am. Chem. Soc.* **1935**, *57*, 202.
(45) Gray, A. P. *Thermochim. Acta* **1970**, *1*, 563.
(46) Arventi, B. I. *Bull. Soc. Chim. Fr.* **1937**, *4*, 999.
(47) (a) Muller, P.; Seres, J.; Steiner, K.; Helali, S. E.; Hardegger, E. *Helv. Chim. Acta* **1974**, *57*, 790. (b) Fieser, L. F.; Fieser, M. *Reagents for Organic Synthesis*; Wiley: New York, 1967; p 964.
(48) Autenrieth, W.; Muhlinghaus, P. *Chem. Ber.* **1907**, *40*, 744.
(49) Leman, A. *Ann. Chim.* **1938**, *9*, 357.
(50) Schönberg, A.; Mustafa, A. *J. Chem. Soc.* **1943**, 79.
(51) Anderson, L. C.; Thomas, D. G. *J. Am. Chem. Soc.* **1943**, *65*, 234.


MA000392U